



Regulation of WNT5A and WNT11 during MSC in vitro chondrogenesis: WNT inhibition lowers BMP and hedgehog activity, and reduces hypertrophy

Solvig Diederichs¹ · Veronika Tonnier¹ · Melanie März¹ · Simon I. Dreher¹ · Andreas Geisbüsch² · Wiltrud Richter¹

Received: 13 February 2019 / Revised: 4 April 2019 / Accepted: 8 April 2019 / Published online: 12 April 2019
© Springer Nature Switzerland AG 2019

Abstract

Re-directing mesenchymal stromal cell (MSC) chondrogenesis towards a non-hypertrophic articular chondrocyte-(AC)-like phenotype is important for improving articular cartilage neogenesis to enhance clinical cartilage repair strategies. This study is the first to demonstrate that high levels of non-canonical WNT5A followed by WNT11 and *LEF1* discriminated MSC chondrogenesis from AC re-differentiation. Moreover, β -catenin seemed incompletely silenced in differentiating MSCs, which altogether suggested a role for WNT signaling in hypertrophic MSC differentiation. WNT inhibition with the small molecule IWP-2 supported MSC chondrogenesis according to elevated proteoglycan deposition and reduced the characteristic upregulation of *BMP4*, *BMP7* and their target *ID1*, as well as *IHH* and its target *GLI1* observed during endochondral differentiation. Along with the pro-hypertrophic transcription factor MEF2C, multiple hypertrophic downstream targets including *IBSP* and alkaline phosphatase activity were reduced by IWP-2, demonstrating that WNT activity drives BMP and hedgehog upregulation, and MSC hypertrophy. WNT inhibition almost matched the strong anti-hypertrophic capacity of pulsed parathyroid hormone-related protein application, and both outperformed suppression of BMP signaling with dorsomorphin, which also reduced cartilage matrix deposition. Yet, hypertrophic marker expression under IWP-2 remained above AC level, and in vivo mineralization and ectopic bone formation were reduced but not eliminated. Overall, the strong anti-hypertrophic effects of IWP-2 involved inhibition but not silencing of pro-hypertrophic BMP and IHH pathways, and more advanced silencing of WNT activity as well as combined application of IHH or BMP antagonists should next be considered to install articular cartilage neogenesis from human MSCs.

Keywords WNT · Mesenchymal stromal cells · Chondrogenesis · Hypertrophy · Cartilage · Bone

Solvig Diederichs and Veronika Tonnier contributed equally to the manuscript.

Electronic supplementary material The online version of this article (<https://doi.org/10.1007/s00018-019-03099-0>) contains supplementary material, which is available to authorized users.

✉ Wiltrud Richter
wiltrud.richter@med.uni-heidelberg.de

¹ Research Center for Experimental Orthopaedics, Heidelberg University Hospital, Heidelberg, Germany

² Clinic for Orthopaedics and Trauma Surgery, Heidelberg University Hospital, Heidelberg, Germany

Introduction

Articular cartilage has a poor regenerative capacity and localized cartilage defects which are left untreated represent a clear risk for development of osteoarthritis [1]. Several surgical techniques are available to stimulate healing of damaged cartilage [2–4] and multiple cell-based strategies have been tested and optimized to reach satisfying outcome after cartilage repair [5]. The clinical use of cell-based therapies relies on autologous chondrocytes harvested from a less load-bearing area of the patients' joint and this tissue damage to obtain articular chondrocytes (ACs) for implantation as well as a rather limited understanding of articular cartilage neogenesis still hampers the development of successful therapies to restore joint surface defects.

Bone marrow-derived mesenchymal stromal cells (MSCs) are an attractive alternate cell source for cartilage

regeneration but when induced to differentiate into chondrocytes in vitro, MSCs recapitulate the endochondral differentiation of growth plate chondrocytes, become hypertrophic and develop an inherent mineralization activity leading to bone formation at ectopic sites [6]. Instead, ACs re-differentiate into a stable articular cartilage phenotype and form no bone under the same conditions [6]. Permanent secretion of parathyroid hormone-related protein (PTHrP) was suggested as a potential mechanism how ACs actively prevent progression to hypertrophy [7] in line with studies on embryonic cartilage development [8, 9]. However, MSCs down-regulate PTHrP expression during early chondrogenesis in favor of upregulation of BMPs and Indian hedgehog (IHH), and progress along the endochondral pathway with common hypertrophic and osteogenic markers being upregulated [7, 10]. The drivers for this BMP and IHH upregulation remain currently unknown.

Re-directing MSC chondrogenesis to obtain stable chondrocytes is an active field of investigation, and to date, a few studies have claimed to achieve a stable, articular cartilage phenotype by in vitro differentiation of MSCs [11–15]. Intriguingly, completely different or even opposite strategies [11, 12] were applied, suggesting the apparent ease of such an attempt. But neither approach, being it WNT signaling stimulation [12], WNT signaling stimulation followed by inhibition [11], selective silencing of a single microRNA [13], silencing of BMP receptor signaling [15], or growing a self-assembling tissue in dual compartment culture [14], has yet independently been reproduced. Neither of these studies addressed whether the obtained MSC-derived chondrocytes indeed copied the low levels of relevant hypertrophic (like COL10A1, IHH, MEF2C and PTH1R) and osteogenic markers (ALPL, IBSP, OPN, RUNX2) of ACs; nor have mechanisms regarding an active or passive maintenance of chondrocyte phenotype stability been considered at all [14] or beyond a single pathway [11–13, 15]. Given the importance and tight interaction of TGF- β , BMP, WNT and IHH signaling pathways during embryonic cartilage development [16], consideration of more than one pathway is required for a comprehensive understanding of articular cartilage neogenesis.

We previously reported that introduction of short daily PTHrP(1–34) pulses during chondrogenesis of MSCs prevents upregulation of *IHH* and keeps the osteogenic markers ALP and *IBSP* and the hypertrophic marker *MEF2C* at lower levels, while slightly increasing cartilage matrix deposition [17]. However, *COL10A1* and *PTH1R* expression were insufficiently reached, indicating that PTHrP(1–34) pulses acted strongly anti-osteogenic but only selectively anti-hypertrophic. Bone morphogenetic proteins (BMPs) are, in addition to their pro-chondrogenic activity, also widely believed to drive chondrocyte hypertrophy [18–20]. In line, MSCs upregulated *BMP4* and *BMP7* expression during

MSC chondrogenesis, while, in turn, ACs increased natural BMP antagonists [21]. However, since BMP signaling was also essential for early SOX9 upregulation, silencing of early canonical BMP signaling with dorsomorphin prevented chondrogenesis, while later treatment suppressed hypertrophy at the expense of reduced differentiation and cartilage matrix deposition [21]. Conclusively, neither PTHrP(1–34) pulses nor dorsomorphin were fully able to shift MSCs from the endochondral development of growth plate chondrocytes to the stable articular chondrocyte phenotype.

WNT signaling controls chondrocyte hypertrophy and endochondral ossification in the growth plate during limb development [22–27]. It consists of a complex network of pathways including the canonical pathway inducing stabilization and nuclear translocation of the transcriptional co-activator β -catenin and several less well-understood non-canonical pathways that act independent of β -catenin. Despite its evident role in cartilage and bone development, surprisingly little is known about WNT activity and regulation of WNT network molecules during endochondral MSC differentiation compared to ACs. Which of the 19 known WNT ligands may contribute to driving MSC hypertrophy, the relevance of canonical versus non-canonical WNT signaling, and whether natural WNT inhibitors may protect ACs from hypertrophy during re-differentiation, are important questions that remain insufficiently understood.

In osteoblasts, WNT signals have been reported to cross-talk with both BMP and IHH signaling. Specifically, induction of ALP activity was synergistically driven by WNT and BMP2 [28, 29] with WNT acting as upstream regulator of BMP expression and ALP activity [30]. WNT/BMP cross-talk was also observed in many other biological processes [28, 31, 32]. Moreover, in growth plate chondrocytes, WNT was reported to act upstream of IHH and inhibit chondrocyte apoptosis [33, 34]. Thus, inhibition of WNT signaling during MSC in vitro chondrogenesis may have the potential to lower BMP and IHH signaling, and repress prominent hypertrophic and osteogenic differentiation markers to levels seen in ACs.

Aim of this study was to identify specific candidate drivers in the complex WNT signaling network and the mechanism by which WNT signaling results in transient endochondral cartilage formation. Here, we hypothesized that WNT activity drives BMP and IHH upregulation during endochondral MSC differentiation and that WNT inhibition could silence both BMP and IHH signaling. Thus, WNT inhibition could potentially be more powerful for re-directing MSC chondrogenesis towards chondrocytes which are resistant to ectopic in vivo mineralization than manipulating either the BMP or IHH pathway alone. Altogether, this will improve articular cartilage neogenesis from MSCs and provide novel therapeutic strategies for regeneration of cartilage tissue in damaged joints.

Materials and methods

Cell isolation, expansion and differentiation

All procedures were in accordance with the ethical standards of the ethics committee on human experimentation of the Medical Faculty of Heidelberg University and with the Helsinki Declaration of 1975 in its latest version. MSCs were isolated from human bone marrow aspirates obtained with informed consent from patients (age 21–83) undergoing total hip replacement. Mononuclear cells were isolated via Ficoll-Paque™ (GE Healthcare) and expanded with Dulbecco's Modified Eagle's Medium (DMEM, Gibco, Life Technologies) high glucose, 12.5% fetal calf serum (FCS, Gibco, Life Technologies), 100 units/ml penicillin, 100 µg/ml streptomycin (Biochrom), 2 mM L-glutamine (Gibco, Life Technologies), 1% non-essential amino acids (Gibco, Life Technologies), 1% β-mercaptoethanol (Gibco, Life Technologies), 4 ng/ml human fibroblast growth factor-2 (FGF-2, Miltenyi Biotec, Germany). Where indicated, 250 ng/ml human recombinant WNT3A (R&D Systems, Germany) was added. In accordance with the generally accepted surface marker profile, our MSCs were routinely tested and found positive for CD90, CD105, CD73 and CD146, and negative for CD34 and CD45 (supplemental figure S7).

ACs were isolated from human articular cartilage obtained with informed consent from patients (age 57–82) undergoing total knee replacement. Cartilage from phenotypically healthy regions was minced and digested overnight at 37 °C with 1.5 mg/ml collagenase B (Roche Diagnostics) and 0.1 mg/ml hyaluronidase (Sigma Aldrich). Chondrocytes were expanded in low-glucose DMEM supplemented with 10% FCS, penicillin/streptomycin.

MSC chondrogenesis and AC re-differentiation were performed in 3D micromass culture by pelleting cells in chondrogenic induction medium (DMEM high glucose, 0.1 mM dexamethasone, 0.17 mM ascorbic acid 2-phosphate, 5 mg/ml transferrin, 5 ng/ml sodium selenite, 1 mM sodium pyruvate, 0.35 mM proline, 1.25 mg/ml BSA (all from Sigma Aldrich), penicillin/streptomycin, 5 mg/ml insulin (Lantus®, Sanofi-Aventis) and 10 ng/ml TGF-β1 (PeproTech). Where indicated, pellets were treated with 2 µM IWP-2 (Tocris Bioscience), or dorsomorphin (10 µM, ENZO Life Science, as described before [21]) starting at day 14 of differentiation. For PTHrP pulse experiments, 2.5 nM PTHrP(1–34) (Bachem) was added starting at day 7 for 6 h before a daily medium exchange, as described previously [17]. Controls received the corresponding amount of solvent.

Microarray analysis

Samples of $n = 4$ AC donors and $n = 5$ MSC donors were studied at day 0 of (re-) differentiation, while $n = 5$ for both ACs and MSCs were used at day 28. Five pellets per population and time point were pooled and total RNA was extracted using RNeasy Mini kit (Qiagen). Microarray analysis (Illumina Human Sentrix, Human Ref_8 v3.0) was performed at the Genomic and Proteomics Core Facility of the German Cancer Research Center in Heidelberg, Germany. Data were extracted for all individual beads and outliers with a more than 2.5-fold difference from the mean were removed. Signals were quantile normalized and log₂ transformed. Group comparisons were performed for 71 identified WNT components, based on the mean signal of all beads per probe passing quality control.

Animal experiments

In vivo mineralization was assessed in the classical ectopic bone formation assay, because subcutaneously, hypertrophic cartilage can become vascularized and remodeled into bone much more quickly than orthotopically in non-vascularized articular cartilage. Importantly, engineered AC-derived cartilage resists vascularization and mineralization at ectopic sites [6]. Experiments were approved by the Animal Experimentation Committee Karlsruhe all procedures were performed according to the national guidelines for animal care in accordance with the European Union Directive (2010/63/EU). 4 day 35 pellets were implanted into subcutaneous pouches of female SCID mice (8–9 weeks old, CB17/Icr-Prkdcscid/IcrIcoCrl Charles River Laboratories, Germany). Animals were anaesthetized by Medetomidine (Sedin® 0.3 mg/kg, Alvetra) and Ketamin® (120 mg/kg, Medistar). One hour after surgery, the anesthesia was antagonized by Atipamezol (Alzane® 2.5 mg/kg, Zoetis). No animal exhibited adverse reactions to the presence of the implants throughout the duration of the experiments and the animals were killed 8 weeks after surgery.

Micro-CT analysis

Pellets were scanned in skin pouches in the Sky-Scan 1076 in vivo X-ray microtomograph (Skyscan) using a 0.5-mm aluminum filter, with the following settings: voxel size 8.85 µm, 48 kV, 200 µA, frame averaging 3. Data were recorded every 1.1° rotation step through 180°. Reconstruction of the X-ray pictures was performed using NRecon® software (version 1.6.3.2, Skyscan). CTAn® software was used for calculating the volume of mineralized tissue in the volume of interest. For analysis of the mineralized volume, the lower gray level was set at 75 and the upper gray level was set at 255. Two pellets (one from the control group, one

from the WNT3A-expanded IWP-2 group) were lost after scanning and could, thus, not be processed for histology.

Histology

Explants were partially decalcified for 1 day in Bouin's solution (Sigma-Aldrich); in vitro pellets were fixated for 2 h in 4% formaldehyde (Merck). 5- μ m paraffin sections were stained according to standard histological procedures with safranin O (0.2% in 1% acetic acid) with fast green counterstaining (0.04% in 0.2% acetic acid), or with Mayer's hematoxylin and eosin counterstaining (1% aqueous solution), or with Movat's pentachrome (all from Chroma). ALP activity on paraffin embedded sections was visualized via turnover of NBT/BCIP (Roche).

For immunohistochemistry, sections were treated with 4 mg/mL hyaluronidase followed by 1 mg/mL pronase (Roche), and unspecific binding sites were blocked with 5% BSA. Collagen II and X were visualized using the same primary antibodies as for Western blotting (see below) and biotinylated goat anti-mouse antibody (1:500; Dianova) followed by streptavidin-alkaline phosphatase and fast red detection (Roche).

Quantitative reverse transcription PCR

Four or five pellets per donor, time point, and condition were pooled and mechanically minced. RNA was extracted via guanidinium thiocyanate/phenol (Trifast, peqGOLD, Peqlab) standard protocol. Poly-adenylated mRNA was extracted using oligo-d(T)-coupled magnetic beads (Dynabeads, Dynal, Thermo Fisher Scientific) and reverse transcribed with Omniscript[®] (Qiagen). Transcript levels were determined via qPCR using Light Cycler[™] technology (Roche Diagnostics) with the primers given in supplemental table S3. Gene expression was calculated relative to the mean expression of the reference genes *CPSF6* and *HNRPH1* via the ΔC_t method. Percent reference gene values were calculated as $100\% \cdot 1.8^{\Delta C_t}$.

Western blotting

Whole cell lysates were prepared using RIPA buffer or PhosphoSafe[™] Extraction Reagent (Novagen, Merck Millipore) supplemented with 1 mM Pefabloc[®] (Sigma-Aldrich). Concentration of proteins was determined via Bradford reagent (Sigma Aldrich) and BSA standards. Collagens were isolated from micromass pellets after pepsin digestion as described previously [7]. Note that most proteins including common reference proteins like actin and GAPDH are degraded by pepsin. Proteins were separated via denaturing SDS-PAGE and blotted onto a nitrocellulose membrane (GE Healthcare). Immunostaining was performed using

the following antibodies: anti-MEF2C (clone D80C1, Cell Signaling, 5030), anti-active β -catenin (clone 8E7, Merck Millipore, 05-665), anti-total β -catenin (BD Biosciences, 610154), anti-WNT11 (Merck Millipore, ABD105), anti-WNT5A (MAB645, R&D systems), anti-pSmad 1/5/8 (Cell Signaling, #9511S), anti-Smad 1 (clone EP565Y, Abcam #33902), anti-Smad 5 (clone EP619Y, Abcam #ab40771), anti- β -actin (clone AC-15, GeneTex, GTX26276), anti-histone H3 (Merck Millipore 07-690), anti-collagen type II (clone 4c11, MP Biomedicals/Quartett), and anti-collagen type X (clone X-53, supernatant provided by Prof. Klaus von der Mark). Endogenous WNT11 or MEF2C in SAOS cells and WNT5A-overexpressing SAOS cells (addgene plasmid #35911, gift from Marian Waterman [35]) served as positive controls. For Smads, MSC-derived chondrocytes served as positive control. Bands were visualized with peroxidase-coupled secondary antibodies using ECL detection.

ALP enzyme activity in the supernatant

Culture supernatants were pooled from 3 pellets per group. 100 μ L supernatant was incubated with 100 μ L substrate [10 mg/mL *p*-nitrophenyl phosphate (Sigma Aldrich) in 0.1 M Glycin (Carl Roth), 1 mM MgCl₂ (Sigma Aldrich), 1 mM ZnCl₂ (Sigma Aldrich), pH 9.6]. Absorbance was measured at 405/490 nm (Sunrise[™], Tecan) and related to a standard curve made from *p*-nitrophenol (Sigma Aldrich) and calculated as ALP activity (ng/mL/min).

GAG and DNA quantification

For measurement of glycosaminoglycan (GAG) and DNA content, two pellets were separately digested with 3 U/mL proteinase K (Fermentas) dissolved in 0.05 M Tris (Merck), 1 mM CaCl₂ (pH 8.0, Sigma Aldrich) overnight at 60 °C. The DNA content of the digest was determined with the Quant iT PicoGreen ds DNA Assay Kit (Thermo Scientific, Germany) and fluorescence was measured at 485/535 nm. For GAG quantification, 30 μ L of the 1:2 diluted proteinase K digest was mixed with 200 μ L 1,9-dimethyl-methylene blue (DMMB, Sigma Aldrich) dye solution (pH 3.0) [36] and absorbance was measured at 530 nm.

Statistics

For all values, mean and standard error of the mean were calculated and differences between groups were analyzed with Student's *t* test for equal or different variances according to *F* test. For comparing MSCs with ACs at the same time points, unpaired analysis was performed, for cells at different time points and for different treatment of cells (IWP-2 vs. control), paired analysis was used. Bonferroni correction was applied to account for multiple testing. Correlation analysis

was performed with Pearson's correlation test. A two-tailed significance value of $p \leq 0.05$ was considered statistically significant.

For microarray analysis (Illumina Human Sentrix, Human Ref_8 v3.0), mean quantile normalized signals of all beads per probe passing quality control signals were calculated.

Results

To document the chondrogenic capacity of MSCs and the differences between endochondral MSC differentiation and AC re-differentiation, we compared expression of specific marker genes and matrix deposition in MSC versus AC cultures on day 28 of (re-) differentiation. Two common chondrogenic, four hypertrophic, and four osteogenic markers were assessed including the pro-hypertrophic transcription factor MEF2C and the pro-osteogenic transcription factor RUNX2 (Table 1). *COL2A1*, *ACAN* and *SOX9* mRNA levels were comparable in chondrocytes derived from both sources, while mean expression of hypertrophy-associated *COL10A1*, *PTH1R*, *IHH* and *MEF2C* was strongly elevated in MSC-derived chondrocytes. The osteogenic markers *SPP1* (osteopontin) and *ALPL* reached about 80-fold higher levels in MSC-derived tissue than in ACs. In a time course over 6 weeks, *COL2A1* upregulation was similar in both groups (supplemental figure S1A) and *ACAN* upregulation in MSCs reached levels in ACs from day 28 on, while hypertrophic and osteogenic markers remained low in ACs. *COL10A1* was significantly higher in MSCs from day 7 onwards (figure S1B), ALP activity from day 14 onwards (figure S1C) and *IHH* from day 21 onwards (figure S1B). Cartilage matrix rich in proteoglycans and collagen type II accumulated in (re-) differentiated AC- and MSC-derived tissue (figure

S1D), while only differentiated MSC-derived chondrocytes deposited collagen type X. Thus, at similar *COL2A1* expression, hypertrophic and osteogenic markers were upregulated exclusively during MSC chondrogenesis.

Enhanced expression of non-canonical WNT ligands in MSC-derived chondrocytes

To discover a differential expression of WNT network members between MSC-derived hypertrophic chondrocytes and re-differentiated ACs, we extracted 71 WNT components from whole-genome transcriptome data obtained from 4 to 5 donor cell populations per group. Importantly, typical canonical WNT ligands were barely expressed in chondrocytes from both groups (supplemental table S1). At day 28, eleven genes showed a more than twofold difference in mean expression levels between re-differentiated ACs and MSC-derived chondrocytes (Table 2). They included the non-canonical ligands *WNT5A* and *WNT11*, the non-canonical (co-) receptors *FZD9* and *PTK7*, two signaling molecules including the canonical transcription factor *LEF1*, as well as four inhibitors and activators comprising the canonical antagonist *SFRP1*. Importantly, nine out of these eleven genes were higher expressed in the MSC-derived chondrocytes, suggesting higher WNT activity specifically in hypertrophic chondrocytes. PCR validation in independent samples largely confirmed higher expression of these genes of interest in hypertrophic chondrocytes (supplemental table S2). Taken together, higher expression of non-canonical ligands and (co-) receptors in MSC-derived chondrocytes suggested a role for non-canonical WNT signaling in hypertrophic differentiation. Nevertheless, according to enhanced expression of canonical *LEF1* and *SFRP1* in the MSC group, canonical WNT signaling may also be important.

Table 1 Mean expression of marker genes at day 28 of MSC chondrogenesis vs. AC re-differentiation ($n=5$ per group) extracted from whole-genome microarray analysis

| Gene | MSC | AC | Fold |
|---|---------|---------|------|
| Chondrogenic | | | |
| <i>SOX9</i> : sex determining region Y-box 9 | 3631.0 | 2289.0 | 1.6 |
| <i>COL2A1</i> : collagen type II | 19762.0 | 20027.9 | -1.0 |
| <i>ACAN</i> : aggrecan | 143.5 | 215.3 | -1.5 |
| Hypertrophic | | | |
| <i>COL10A1</i> : collagen type X | 13370.0 | 495.5 | 27.0 |
| <i>PTH1R</i> : parathyroid hormone receptor 1 | 10026.3 | 1007.2 | 10.0 |
| <i>IHH</i> : indian hedgehog | 180.0 | b | 3.0 |
| <i>MEF2C</i> : myocyte enhancer factor 2C | 460.1 | 179.6 | 2.6 |
| Osteogenic | | | |
| <i>SPP1</i> : secreted phosphoprotein 1 (osteopontin) | 10720.8 | 132.4 | 81.0 |
| <i>ALPL</i> : alkaline phosphatase | 9304.0 | 122.1 | 76.2 |
| <i>IBSP</i> : integrin-binding sialoprotein | 3169.6 | b | 48.5 |
| <i>RUNX2</i> : runt-related transcription factor 2 | 410.6 | 145.3 | 2.8 |

b mean values are below background (80)

Table 2 Mean *WNT* component expression at day 28 of MSC chondrogenesis vs. AC re-differentiation extracted from microarray data ($n=5$)

| Gene | MSC | AC | Fold |
|---|--------|-------|------|
| Ligands | | | |
| <i>WNT5A</i> : wingless-type MMTV integration site family, 5A | 309.4 | 155.2 | 2.0 |
| <i>WNT11</i> : wingless-type MMTV integration site family, 11 | 292.2 | 111.6 | 2.6 |
| Receptors | | | |
| <i>FZD2</i> : frizzled homolog 2 | 192.3 | 89.4 | 2.2 |
| <i>FZD9</i> : frizzled homolog 9 | 1086.0 | 545.6 | 2.0 |
| Co-receptors | | | |
| <i>PTK7</i> : protein tyrosine kinase 7 | 1145.1 | 288.9 | 4.0 |
| Signaling molecules | | | |
| <i>LEF1</i> : lymphoid enhancer binding factor 1 | 1157.6 | 207.4 | 5.6 |
| <i>PRICKLE1</i> : prickle homolog 1 | 904.9 | 203.6 | 4.4 |
| Inhibitors/activators | | | |
| <i>SFRP1</i> : secreted frizzled-related protein 1 | 1452.6 | 105.4 | 13.8 |
| <i>APCDD1</i> : adenomatosis polyposis coli down-regulated 1 | 549.4 | 239.5 | 2.3 |
| <i>RSPO2</i> : R-spondin 2 homolog | 129.5 | 316.2 | -2.4 |
| <i>RSPO3</i> : R-spondin 3 homolog | 165.2 | 894.8 | -5.4 |

Only genes with a \geq twofold difference are listed

Inverse regulation of *WNT5A* and *WNT11* during MSC chondrogenesis

Interestingly, *WNT5A* and *WNT11*, the two ligands found above to be expressed during MSC chondrogenesis, are also the prevailing *WNT* ligands in growth plate chondrocytes [37]. Therefore, we were interested in their regulation during endochondral MSC differentiation. *WNT11* was significantly upregulated during MSC chondrogenesis from day 7 on, reaching significantly higher mRNA levels than re-differentiated ACs from day 21 on ($p < 0.05$; Fig. 1a). Western blotting confirmed this upregulation during MSC chondrogenesis (Fig. 1b; $n=2-4$), while *WNT11* remained undetectable in ACs (not shown). By contrast, mean *WNT5A* expression was higher in MSCs than in ACs at day 0 and *WNT5A* became significantly downregulated during MSC chondrogenesis ($p < 0.05$; Fig. 1a), while it remained low during AC re-differentiation. In line, Western blotting detected *WNT5A* protein in MSCs but not ACs at day 0 (Fig. 1b, $n=3-4$) demonstrating that only MSCs started into chondrogenesis with high *WNT5A* levels.

Along with non-canonical *WNT11*, the non-canonical (co-) receptors *FZD9* and *PTK7* were significantly upregulated only during MSC chondrogenesis (Fig. 1c). In addition, the canonical transcription factor *LEF1* increased significantly, reaching 8.5-fold higher levels than in ACs at day 35, while the canonical antagonist *SFRP1*, although not upregulated, remained significantly higher in MSC-derived chondrocytes than in re-differentiated ACs (19.7-fold on day 35, $p < 0.05$).

High active β -catenin levels were observed by Western blotting on day 0 in both groups which gradually declined

over time. However, a slightly slower drop in the MSC group suggested a trend for higher canonical *WNT* activity in hypertrophic chondrocytes (Fig. 1d). In summary, regulation of non-canonical *WNT5A* and *WNT11* ligands and specific upregulation of non-canonical *FZD9* and *PTK7* with hypertrophy provided strong arguments for a relevance of non-canonical *WNT* signaling during MSC chondrogenesis, with the β -catenin-dependent canonical pathway being also involved.

Strong anti-osteogenic and mild anti-hypertrophic effects of *WNT* inhibition

To test whether inhibition of *WNT* signaling can re-direct MSC chondrogenesis to obtain stable chondrocytes, we blocked processing and secretion of all *WNT* ligands by the porcupine inhibitor IWP-2 to silence canonical and non-canonical signaling. The reduced levels of the canonical *WNT* response gene *AXIN2* under IWP-2 compared to DMSO controls confirmed a reduced canonical *WNT* activity on days 21 and 35, i.e., after 1 and 3 weeks of treatment (supplemental figure S2A). Chondrogenic differentiation of MSCs remained high under IWP-2 according to maintained *SOX9*, *COL2A1*, and *ACAN* expression and similar safranin O and collagen type II staining of pellets (figure S2A,B). GAG/DNA content was slightly but significantly increased under IWP-2 (1.2-fold, $p < 0.05$; figure S2C), suggesting a slight anabolic effect of *WNT* inhibition.

A mild anti-hypertrophic effect was observed on the expression of all four tested markers (*COL10A1*, *IHH*, *PTH1R*, *MEF2C*), which remained significantly lower under IWP-2 ($p < 0.05$; Fig. 2a). For *PTH1R*, the day 35 effect

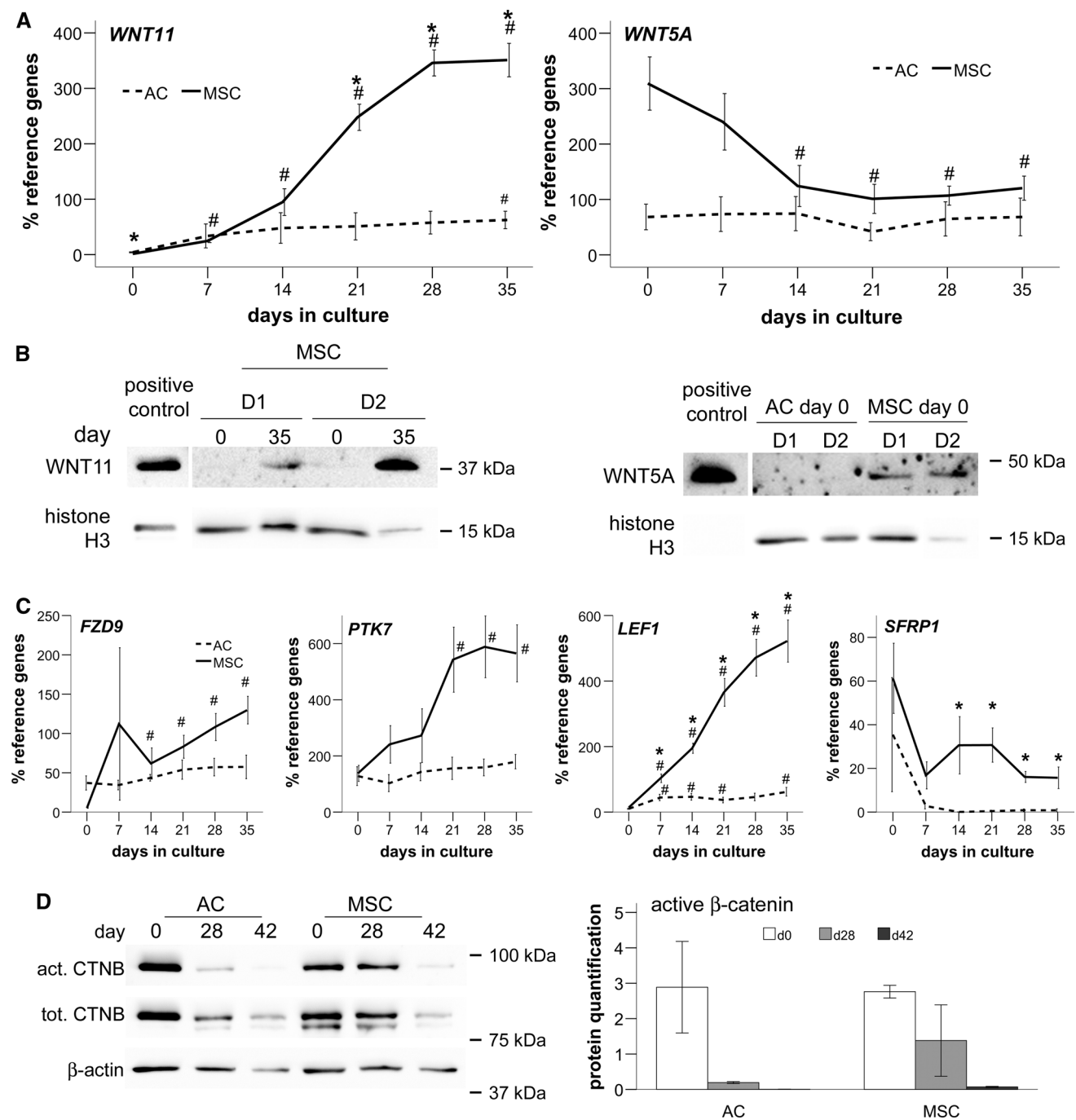


Fig. 1 Inverse regulation of WNT11 and WNT5A and downregulation of β -catenin during MSC chondrogenesis. Micromass pellets of ACs and MSCs were cultured for up to 6 weeks in chondrogenic medium with TGF- β . **a** qPCR assessment of the regulation of gene expression over time (mean \pm SEM of $n=5$ independent donor populations of ACs and MSCs). *HNRPH1* and *CPSF6* were used as reference genes. * $p < 0.05$ vs. AC at the same time point; # $p < 0.05$ vs. day 0. **b** WNT11 at days 0 and 35 in 2 representative out of 4 independent

MSC populations with histone H3 as reference; and WNT5A at day 0 in independent AC and MSC populations (D1, D2, representative for $n=3-4$). **c** Gene expression relative to *HNRPH1* and *CPSF6* depicted as mean \pm SEM of $n=5$ independent donor populations with * $p < 0.05$ vs. AC at the same time point and # $p < 0.05$ vs. day 0. **d** Active and total β -catenin with β -actin as reference. One representative blot of 3 independent experiments shown. Quantification of β -catenin blots relative to β -actin

was only seen by trend. Although *COL10A1* mRNA levels remained 20–30% lower, the collagen type X content per pellet was maintained under IWP-2 as was collagen type II

deposition (Fig. 2c). In line with reduced *MEF2C* mRNA expression (Fig. 2a), protein levels of MEF2C were lower under IWP-2 (Fig. 2d), suggesting that WNT signaling

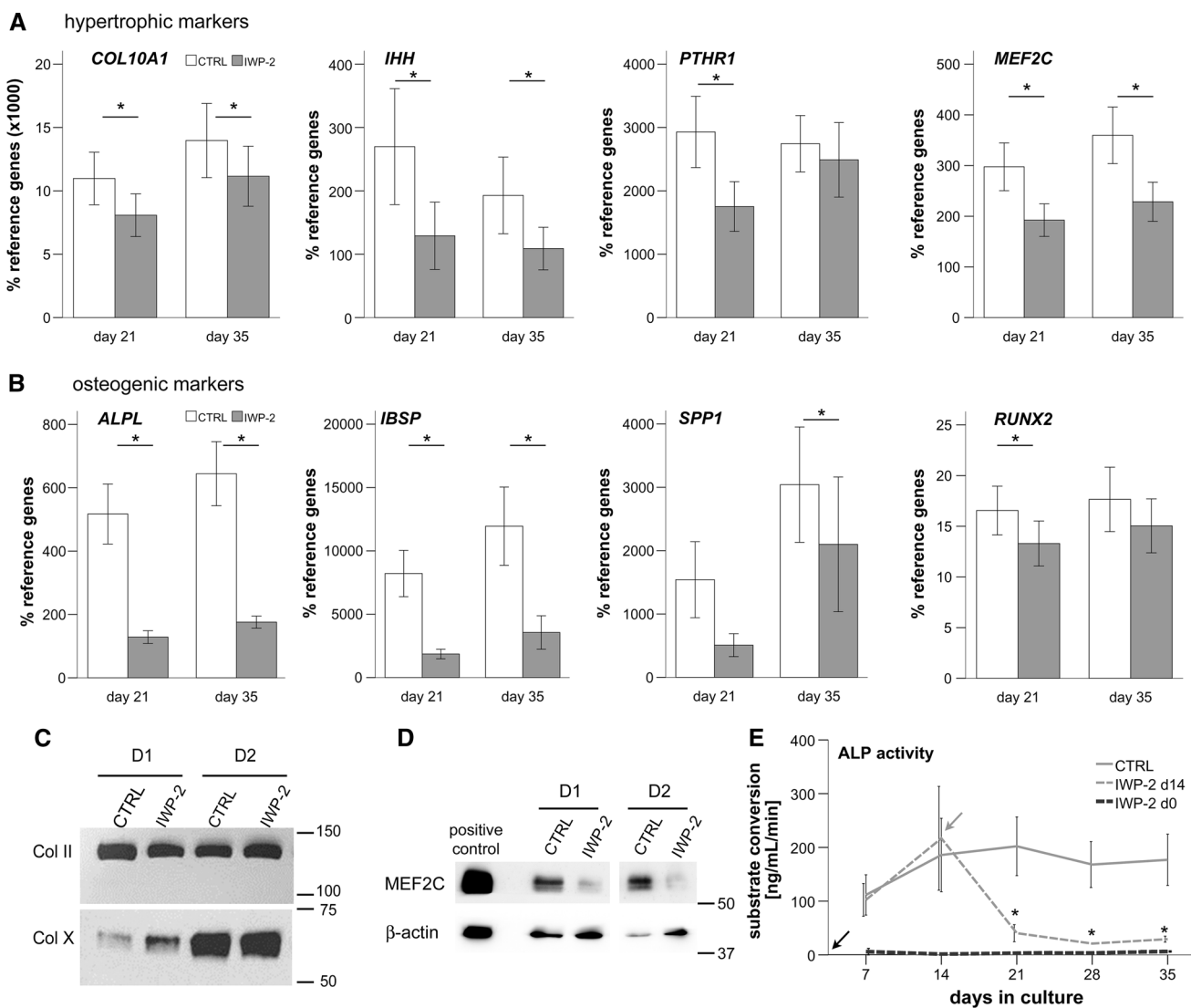


Fig. 2 WNT inhibition suppresses mineralizing activity developing during MSC chondrogenesis. Micromass MSC pellets were cultured for up to 5 weeks in chondrogenic medium with TGF- β . Treatment with 2 μ M IWP-2 or DMSO as control was started at day 14. **a**, **b** qPCR assessment of specified hypertrophic and osteogenic markers. Depicted is the mean \pm SEM of $n=5$ independent donor populations; $*p < 0.05$ CTRL vs. IWP-2 at the same time point. **c** Western blot of collagen types II and X in precipitates of day 35 micromass cultures of 2 independent MSC populations (D1, D2). Equal volumes of re-

solved collagen precipitates were loaded. **d** MEF2C Western blot in cell lysates of day 35 micromass cultures of 2 independent MSC populations (D1, D2). **e**: ALP activity in the supernatant measured by conversion of the substrate *p*-nitrophenylphosphate (mean \pm SEM; $n=5$ independent donor populations; $*p < 0.05$ vs. CTRL at the same time point). Two independent experiments were performed with IWP-2 treatments starting at day 0 (gray line). Arrows designate begin of treatment with IWP-2

drives MEF2C upregulation during MSC chondrogenesis. In contrast to mild effects on hypertrophic markers, expression of the osteogenic markers *ALPL* and *IBSP* was strongly suppressed by IWP-2 ($p < 0.05$; Fig. 2b) and *SPP1* and *RUNX2* were also affected. Importantly, ALP activity was strongly downregulated by IWP-2 by about 80% on days 21–35 (Fig. 2e). Constant suppression of ALP activity at maintained chondrogenic capacity was obtained, when IWP-2 treatment was started at day 0 of MSC chondrogenesis ($n=2$, Fig. 2e).

Since an earlier study reported generation of stable chondrocytes when MSCs were expanded under WNT3A treatment before IWP-2 was applied during chondrogenesis, we repeated our experiments with WNT3A-expanded MSCs, following the conditions described by Narcisi et al. [11]. Prior WNT3A application did largely not affect the outcome seen with IWP-2 treatment alone; although due to lower replicate numbers ($n=3$ independent experiments), some effects remained only by trend (supplemental figure S3).

Conclusively, IWP-2 strongly suppressed ALP activity relevant for tissue mineralization and reduced osteogenic markers during MSC chondrogenesis, indicating a strong anti-osteogenic activity of IWP-2. In contrast, hypertrophic markers were only mildly affected and collagen type X protein deposition appeared unchanged by IWP-2. These effects were independent of pre-stimulation by WNT3A.

Co-regulation of WNT11 with MEF2C, IBSP and ALPL

Hypothesizing that expression levels of a driver of MSC hypertrophy would correlate with levels of hypertrophic/osteogenic markers, we assessed some WNT genes of interest for correlated expression with the three marker genes *MEF2C*, *ALPL*, and *IBSP*, which were most strongly reduced by IWP-2. Importantly, only *WNT11* levels, but not *WNT5A*, *FZD9*, *PTK7*, and *LEF1* levels showed a significant

positive correlation with all three tested marker genes with the highest correlation coefficient seen between *WNT11* and *MEF2C* ($\rho = 0.936$, $p < 0.0001$; Fig. 3a), followed by *IBSP* ($\rho = 0.859$, $p < 0.0001$). This suggested that *WNT11* expression is linked with the prominent pro-hypertrophic transcription factor *MEF2C* [38, 39] and its downstream targets *IBSP* and *ALPL* [40]. Whether WNT11 directly drives *MEF2C* expression, or vice versa, should next be determined by over-expression studies.

WNT inhibition lowers BMP and IHH target gene expression

Asking whether WNT signaling during MSC in vitro chondrogenesis may drive BMP and IHH signaling, we investigated whether the known upregulation of *BMP4* and *BMP7* during MSC chondrogenesis [21] and expression of the

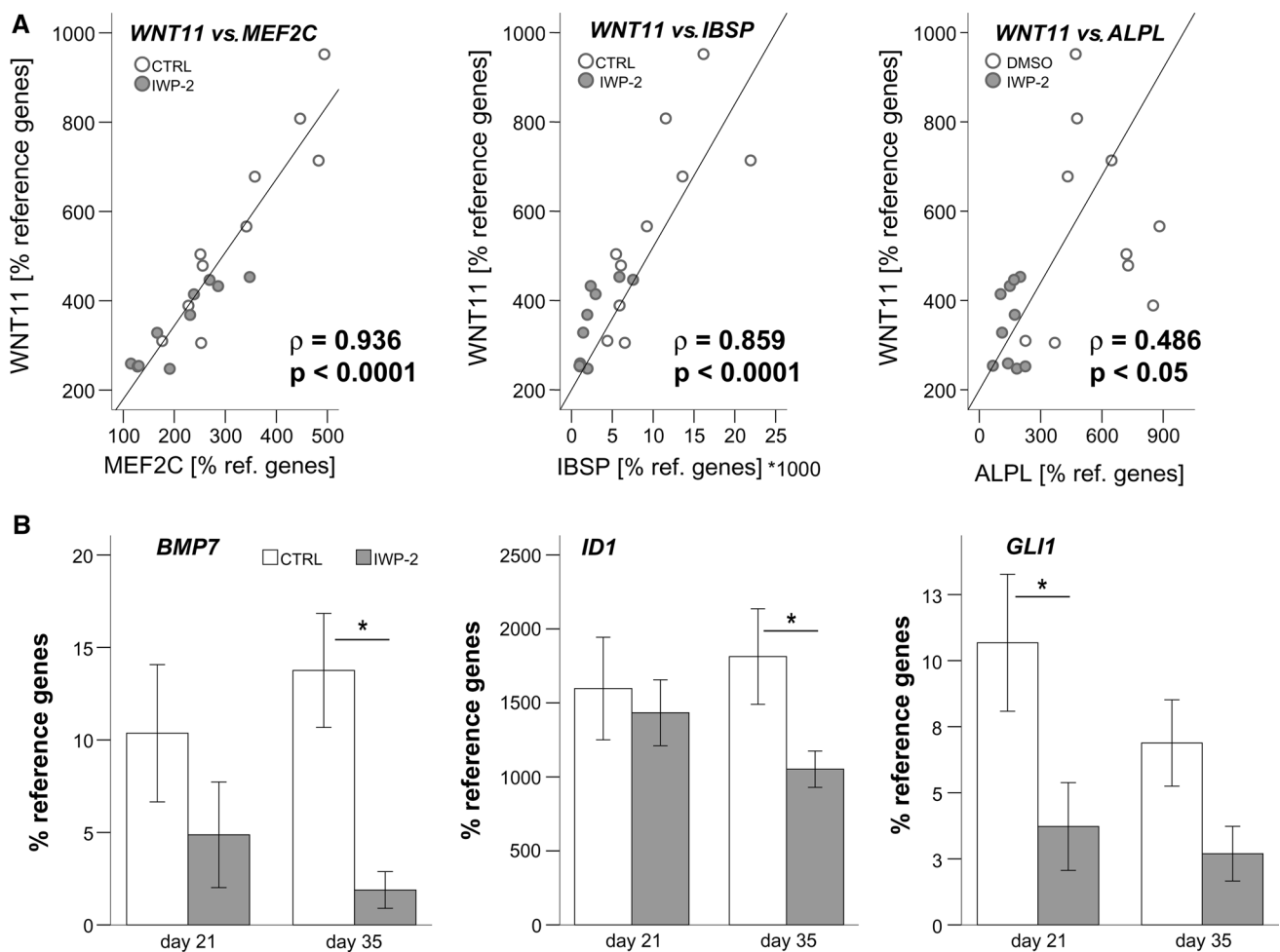


Fig. 3 Correlation of *WNT11* with hypertrophic/osteogenic markers and suppression of BMP- and IHH targets by WNT inhibition. **A**: Micromass pellets of MSCs were treated with 2 μ M IWP-2 or the respective amount of DMSO as control starting at day 14 of chondrogenic culture in the presence of TGF- β . Pearson correlation of

WNT11 with expression of *ALPL*, *IBSP*, and *MEF2C* after chondrogenesis ($n = 20$ from 5 independent populations). **B** qPCR assessment of specified genes at day 21 and day 35. Data are presented as mean \pm SEM of $n = 5$ independent populations

common BMP target gene *ID1* [41, 42] would be affected by IWP-2 treatment. In line with a crosstalk of WNT signaling with BMP induction, WNT inhibition significantly lowered *BMP4* expression at day 21 (not shown) and *BMP7* expression at day 35 (Fig. 3b). Significant suppression of *ID1* at day 35 indicated an overall reduced activity of the BMP signaling pathway under WNT inhibition (Fig. 3b). Furthermore, along with reduced *IHH* expression (Fig. 2a), the common *IHH* target gene *GLI1* [9] was reduced under IWP-2, demonstrating that WNT inhibition also reduced *IHH* signaling (Fig. 3b). Taken together, this provided strong evidence that WNT signaling drives BMP and *IHH* upregulation during endochondral differentiation of MSCs. This led to the question whether WNT inhibition may be most powerful in re-directing MSC chondrogenesis towards the low marker levels observed in ACs.

Similar effects of WNT inhibition and pulsed PTHrP

We next compared, whether treatment with IWP-2, pulses of the natural *IHH* inhibitor PTHrP(1–34), or application of dorsomorphin to silence BMP signaling would suppress hypertrophic and osteogenic markers to levels observed in ACs. As expected, dorsomorphin reduced activation

of SMAD1/5/9 during MSC differentiation compared to controls (supplemental figure S4). In line with our previous results [21], dorsomorphin treatment but not pulsed PTHrP(1–34) [43] or IWP-2 was anti-chondrogenic according to strongly reduced *COL2A1* mRNA (Fig. 4a). Notably, hypertrophic and osteogenic markers still remained significantly higher than in re-differentiated ACs under any of the tested conditions (Fig. 4b, c), with one exception. ALP activity was always strongly suppressed reaching levels close to AC niveau (Fig. 4d). Interestingly, *IHH* and *MEF2C* were significantly lower under PTHrP(1–34) pulses than under IWP-2; while otherwise, these two anti-hypertrophic agents resulted overall in a very similar marker profile. Importantly, both treatments outperformed BMP silencing with dorsomorphin which proved anti-chondrogenic. Thus, pulsed PTHrP was more powerful to re-direct MSC chondrogenesis towards an AC expression profile, although effects of IWP-2 came close.

Reduced but not eliminated in vivo mineralization after WNT inhibition

Since ALP levels during MSC chondrogenesis under IWP-2 treatment were as low as in ACs, we tested whether

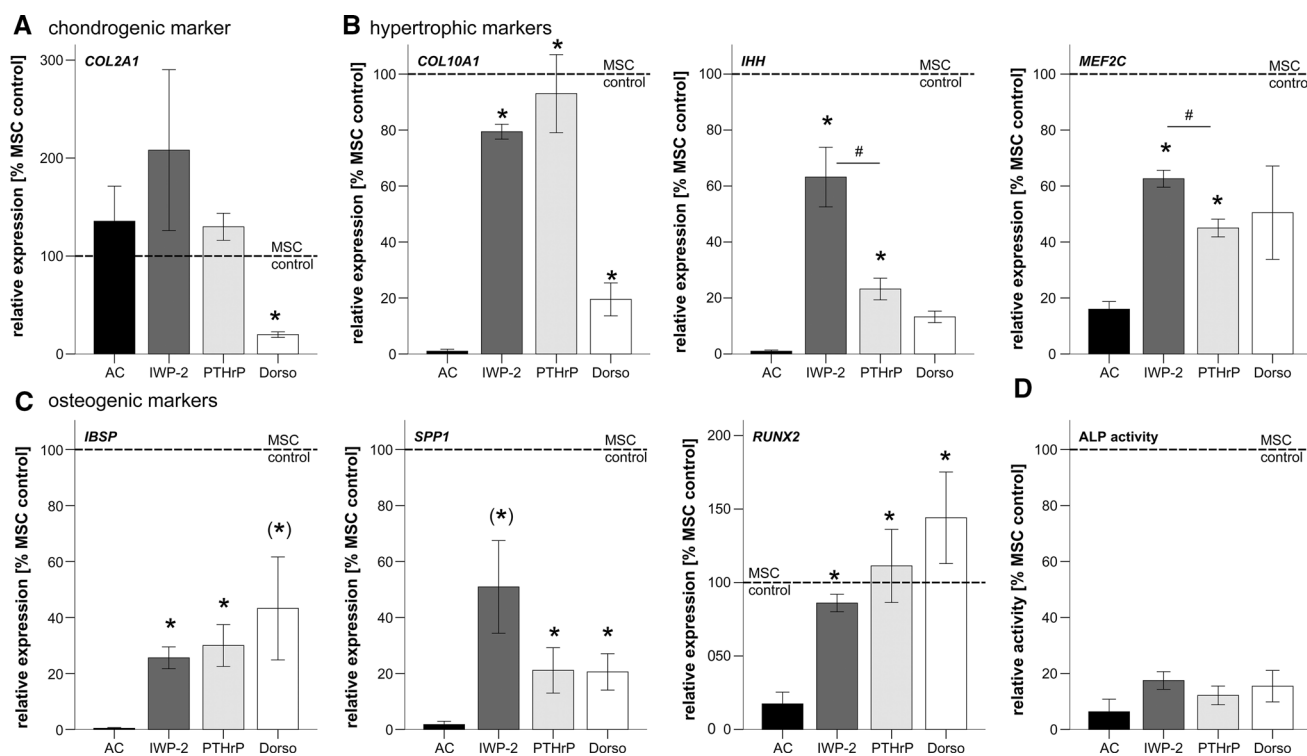


Fig. 4 Comparison of re-differentiated ACs with MSC-derived chondrocytes under treatment with IWP-2, pulsed PTHrP, or BMP silencing with dorsomorphin with regard to chondrogenic, hypertrophic and osteogenic marker expression. qPCR assessment of specified chondrogenic (a), hypertrophic (b) and osteogenic (c) markers as well

as ALP activity (d) in the supernatant at the end of chondrogenesis. Expression of MSC control pellets treated with the respective solvent in chondrogenic medium was set to 100% (dashed line). Mean \pm SEM of $n=3-5$ independent donor populations. * $p < 0.05$ vs. ACs; (*) significance lost by Bonferroni correction; # $p < 0.05$ IWP-2 vs. PTHrP

WNT inhibition would prevent ectopic cartilage mineralization and bone formation as reported for two donors by Narcisi et al. in a recent study [11]. Day-35 MSC pellets generated in the presence or absence of IWP-2 were implanted into subcutaneous pouches of immune deficient mice. Micro-CT analysis revealed mineralization in all 8-week explants from four donors ($n = 24$) (supplemental figure S5). However, in the IWP-2 group, the volume of mineralized tissue was 30% lower (Fig. 5a, b, $p < 0.05$) demonstrating that generation of MSC-derived chondrocytes under WNT inhibition reduced but did not prevent in vivo mineralization. Less mineral deposition under IWP-2 was also observed with WNT3A-expanded MSCs, but due to two outliers, this did not reach significance (supplemental figure S6). This discrepancy to the Narcisi study may be attributed to their use of atypical CD146-negative MSCs, while our MSCs generally contained 60–80% of cells positive for this stem cell potency marker (supplemental figure S7).

According to histology, bone tissue was formed in both, IWP-2-treated samples and controls (4 out of 12 IWP-2 constructs, 7 out of 11 controls, Fig. 5c). Prior WNT3A stimulation did not change these results (bone identified in 5 out of 8 IWP-2 pellets and 6 out of 9 controls, supplemental figure S6c). Taken together, WNT activity drove BMP and IHH upregulation during endochondral MSC development along with MEF2C and hypertrophic downstream targets. However, inhibition of WNT ligand secretion by IWP-2 alone installed no full lineage shift into a permanent articular

chondrocyte phenotype and further WNT blocking options should be considered in the future.

Discussion

Co-induction of hypertrophic and osteogenic markers during MSC in vitro chondrogenesis recapitulates endochondral development of growth plate chondrocytes and pre-determines that the generated cartilaginous tissue becomes mineralized and remodeled into bone at ectopic sites. This is undesired for cartilage regeneration, but the signals that drive MSCs into endochondral development are still incompletely understood. We here showed for the first time that MSC chondrogenesis differed from AC re-differentiation in an incomplete silencing of active β -catenin levels and an inverse regulation of non-canonical WNT5A and WNT11 over time, which interestingly resembled the inverse regulation of PTHrP and IHH during endochondral differentiation. Importantly, we showed that endogenous WNT activity drove MSC hypertrophy and upregulation of BMP and IHH signaling, raising the pro-hypertrophic transcription factor MEF2C along with multiple hypertrophic and especially osteogenic downstream targets. The effect of WNT inhibition was highly similar to pulsed PTHrP(1–34) application, the currently most potent anti-hypertrophic treatment in our hands. As consequence of potent but incomplete suppression of hypertrophy by WNT inhibition in vitro, the generated cartilage tissue mineralized less and formed less ectopic

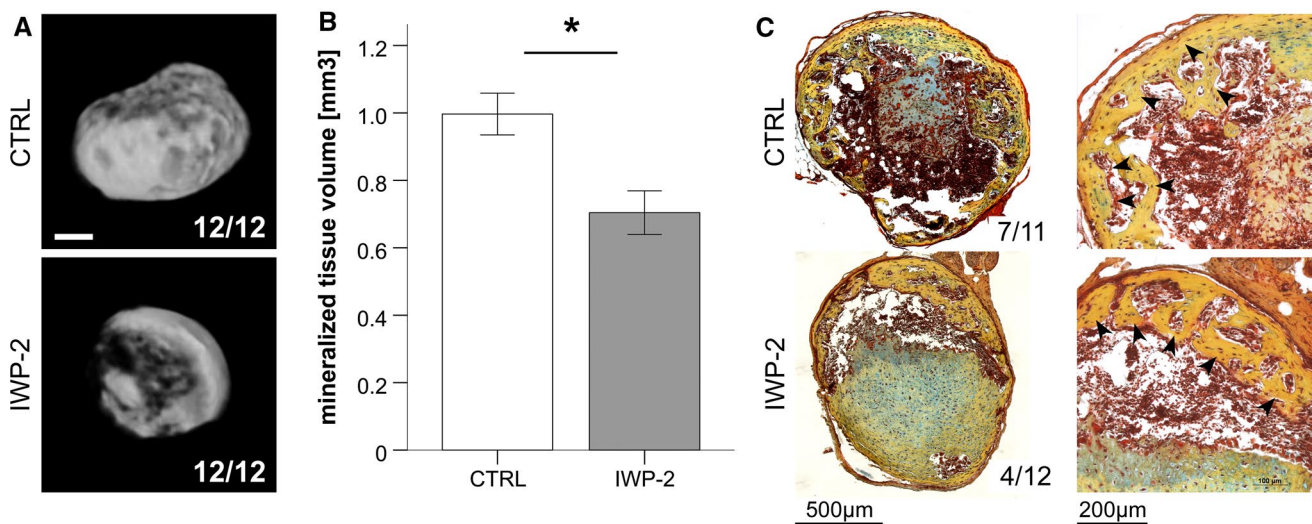


Fig. 5 WNT suppression decreases in vivo mineralization and bone formation. Micromass pellets of MSCs were treated with 2 μ M IWP-2 or the respective amount of DMSO as control starting at day 14 of chondrogenic culture in the presence of TGF- β . After 35 days, 12 micromasses from 4 independent populations per group were implanted subcutaneously into SCID mice. Mice were killed after

8 weeks. **a, b** Micro-CT evaluation of the mineralized tissue volume. Numbers in **a** give the number of mineralized constructs per total construct number, scale bar represents 500 μ m. Data in **b** are given as mean \pm SEM. **c** Movat's pentachrome staining to identify bona fide bone tissue (marked by arrow heads). Numbers refer to the number of samples that formed bone in vivo

bone in vivo than untreated MSC-derived tissue. This demonstrated the importance of endogenous WNT activity for stimulation of MSC hypertrophy and subsequent cartilage mineralization and bone transition in vivo. Importantly, inhibition of WNT ligand secretion by IWP-2 was encouraging but insufficient to fully shift MSC chondrogenesis towards stable ACs. Thus, next aims are to uncover whether more advanced WNT silencing by the use of alternate WNT inhibitors and/or receptor antagonists or a combination of WNT silencing and *IHH* and/or *BMP* silencing is needed to install articular cartilage neogenesis from MSCs.

An important novelty of this study was to pin down WNT ligands and network molecules associated with MSC hypertrophy. The two non-canonical ligands, *WNT5A* and *WNT11*, which were higher expressed during MSC chondrogenesis than in AC re-differentiation, are known to be expressed together with *Wnt5b* and *Wnt4a* in mouse and chick growth plate cartilage [37, 44–46]. Of note, *WNT5B* was also expressed in MSCs and ACs according to our array data, albeit not differentially. Thus, in vitro MSC chondrogenesis, beyond recapitulating many aspects of growth plate development [47], also shared expression of these WNT ligands and is, thus, an attractive model to shed more light on the role of *WNT5A* and *WNT11* for endochondral differentiation.

Typical WNT inhibitors were not higher expressed during AC re-differentiation versus MSC chondrogenesis with exception of *FRZB*, which had previously been implicated in AC phenotype stability [18]. Although fivefold higher expressed in ACs versus MSCs at day 0 (supplemental table S1, PCR confirmation not shown), this difference disappeared during (re-) differentiation. Since other canonical WNT inhibitors like *SFRP1* were even higher in the MSC group, natural WNT inhibitors seemed no relevant protectors from hypertrophy in ACs. This is different in the *BMP* signaling pathway where *BMP* inhibitors were higher expressed in re-differentiating ACs and appeared to help protecting ACs from progression into hypertrophy [21].

Our aim to identify specific WNT drivers of MSC hypertrophy and to illuminate the relevance of canonical versus non-canonical WNT signaling proved unexpectedly difficult. Given the strong evidence for canonical WNT signaling controlling chondrocyte hypertrophy in the mouse growth plate [24–26], we were surprised to find active β -catenin down-regulated when hypertrophic markers were induced during MSC chondrogenesis, and also, the difference in active β -catenin to re-differentiating ACs was surprisingly small. Nevertheless, three previous studies suggested that canonical WNT activity contributed to *ALPL* expression during MSC chondrogenesis, however, without addressing active β -catenin levels [18, 48, 49]. In line with a role of canonical WNT signaling for hypertrophy, IWP-2 here lowered canonical *AXIN2* expression, indicating that reduction of canonical WNT activity may have contributed to redirecting the

chondrocyte phenotype. Being the only ligands differentially expressed during MSC chondrogenesis compared to AC re-differentiation, we propose *WNT5A* and *WNT11* as source for relevant WNT activity.

Wnt5a is one of the most dominant Wnt ligands in mouse and chick limb mesenchyme and growth plate cartilage [50–52]. Mouse knockout studies indicated that *Wnt5a* inhibited chondrocyte proliferation and enhanced progression towards pre-hypertrophic chondrocytes [52, 53], which supports a pro-hypertrophic role of the here observed *WNT5A* expression during early MSC chondrogenesis.

A potential pro-hypertrophic/pro-osteogenic activity of *WNT11* was suggested due to elevated levels observed in pre-hypertrophic chondrocytes underlying the presumptive bone collar in embryonic chick wings [45]. Furthermore, *WNT11* expression correlated with aortic valve calcification which is thought to recapitulate bone development [54]. *Wnt11* overexpression also enhanced ALP activity and osteogenic marker expression in MC3T3-E1 cells and in rat MSCs [55, 56] but not in chicken limb bud cultures and C2C12 cells [45, 57]. Such inconsistencies may be explained by a permissive rather than an active signaling role of *WNT11* as suggested from *Xenopus* studies, where *WNT11* depended on cooperation with instructive TGF- β signaling [58]. Thus, *WNT11* may not cause hypertrophy itself but may be a TGF- β response gene, co-regulated with hypertrophic markers without actively driving them. Quick upregulation upon TGF- β stimulation in MSCs, upregulation also during AC re-differentiation (albeit only 15-fold compared to > 250-fold in MSCs), and mouse studies reporting *Wnt11* as TGF- β target gene [59, 60] support this interpretation. Taken together, *WNT11* may or may not have own pro-hypertrophic activity but may cooperate with other pro-hypertrophic pathways like TGF- β /*BMP*/*Nodal*/*Activin* or *Notch* signaling. This interesting question should be addressed in follow-up studies combining *WNT11* treatment with respective pathway modulators.

Importantly, we here discovered that WNT inhibition during MSC chondrogenesis decreased *BMP* and *IHH* signaling, demonstrating for the first time that WNT, *IHH* and *BMP* formed a pro-hypertrophic network during MSC in vitro chondrogenesis. WNT appeared here to enhance *BMP4* and *BMP7* expression, consistent with WNT/ β -catenin-induced *Bmp2* expression and *BMP* reporter activity in various osteoblastic mouse cells [30].

WNT suppression also reduced *IHH* expression and *IHH* activity, which was no direct IWP-2-mediated effect, since IWP-2 blocks porcupine but not hedgehog acyltransferases [61]. WNT enhancing *IHH* expression was in line with genetic mouse studies showing that Wnt can act upstream of *Ihh* in pre-hypertrophic and hypertrophic growth plate chondrocyte [33, 34]. Importantly, in here, IWP-2 did not fully suppress *BMP* and *IHH* activity, indicating that a

combinatorial inhibitor approach may be necessary to fully silence this pro-hypertrophic network during MSC chondrogenesis, considering also additional, yet unidentified drivers. Extending previous work [47, 62, 63], we recommend MSC chondrogenesis as a valuable human cell-based in vitro model of growth plate development to dissect the contribution of individual signaling pathways and their crosstalk for endochondral cell differentiation.

Effects of WNT inhibition were surprisingly similar to pulsed treatment with PTHrP, which was also strongly anti-osteogenic but only selectively anti-hypertrophic. One likely explanation was that PTHrP pulses acted upstream of WNT activity as demonstrated for bone anabolism, where intermittent PTH regulated WNT activity [32]. In line, pulsed PTHrP treatment lowered *AXIN2* expression in our model similar to IWP-2 (unpublished data). Alternatively, WNT and PTHrP signal transduction may overlap, since both WNT and PTHrP signal via G-protein-coupled receptors that can modulate calcium signaling. Taken together, WNT inhibition and PTHrP pulses probably anastomose, and thus elicit very similar effects.

Our data directly contradicted results from Narcisi et al. [11] who claimed that WNT stimulation during MSC expansion followed by WNT inhibition during chondrogenesis reliably prevented in vivo mineralization of differentiated MSC-derived cartilage. Even inferior MSC donor populations that deposited less proteoglycans and did consequently not form bone in vivo still mineralized the cartilage. Notably, Narcisi et al. worked with MSCs which were negative for CD146, an important potency marker defining the stem cell entity of MSC populations [64, 65]. Thus, Narcisi may have used rather atypical MSC populations which even needed WNT3A treatment for proper expansion. In turn, our MSCs standardly contain 60–80% CD146-positive cells [66] and WNT3A application during expansion did not open means to improve chondrogenesis. In view of the here-shown incomplete silencing of the pro-hypertrophic signaling network in MSCs by all tested treatments and given the discontinuation of inhibition after ectopic transplantation, in vivo mineralization was an expected result. Complete and enduring inhibition of the pro-hypertrophic signaling network requires installation of more potent suppression than achieved here with IWP-2, together with yet-to-define epigenetic memory mechanisms arresting the cells in the AC phenotype.

In conclusion, we here discovered a reciprocal regulation of WNT5A and WNT11 during MSC chondrogenesis and demonstrated that WNT activity drives BMP and IHH upregulation, and hypertrophy during endochondral development, and affected cartilage mineralization and bone transition in vivo. Although in vitro ALP activity was easy to suppress with several anti-hypertrophic treatments including WNT inhibition, fully reprogramming MSC-derived chondrocytes into non-mineralizing ACs remained challenging

and not as simple as some studies had implicated [11, 12]. Since both WNT and PTHrP signal via G-protein-coupled receptors that can modulate calcium signaling, future work should consider the use of corresponding receptor antagonists and alternate WNT inhibitors to govern hypertrophy of MSCs and install articular cartilage neogenesis from MSCs.

Acknowledgements We thank the microarray unit of the DKFZ Genomics and Proteomics Core Facility for providing the Illumina Whole-Genome Expression Beadchips and related services. We also thank Birgit Frey, Jennifer Reimold, Nina Hofmann, Franziska Heilmann, Felicia Klampfleuthner, and Ursula Kreuser for technical assistance and Svitlana Melnik for critical discussions.

References

- Buckwalter JA, Mankin HJ (1997) Articular cartilage. 2. Degeneration and osteoarthritis, repair, regeneration, and transplantation. *J Bone Jt Surg Am* 79A:612–632. <https://doi.org/10.2106/00004623-199704000-00022>
- Huey DJ, Hu JC, Athanasiou KA (2012) Unlike bone, cartilage regeneration remains elusive. *Science* 338:917–921. <https://doi.org/10.1126/science.1222454>
- Makris EA, Gomoll AH, Malizos KN, Hu JC, Athanasiou KA (2015) Repair and tissue engineering techniques for articular cartilage. *Nat Rev Rheumatol* 11:21–34. <https://doi.org/10.1038/nrrheum.2014.157>
- Niemeyer P, Andereya S, Angele P, Ateschrang A, Aurich M, Baumann M, Behrens P, Bosch U, Erggelet C, Fickert S, Fritz J, Gebhard H, Gelse K, Gunther D, Hoberg A, Kasten P, Kolombe T, Madry H, Marlovits S, Meenen NM, Muller PE, Noth U, Petersen JP, Pietschmann M, Richter W, Rolauff B, Rhunau K, Schewe B, Steinert A, Steinwachs MR, Welsch GH, Zinser W, Albrecht D (2013) Autologous chondrocyte implantation (ACI) for cartilage defects of the knee: a guideline by the working group “Tissue Regeneration” of the German Society of Orthopaedic Surgery and Traumatology (DGOU). *Z Orthop Unfall* 151:38–47. <https://doi.org/10.1055/s-0032-1328207>
- Niemeyer P, Porichis S, Steinwachs M, Erggelet C, Kreuz PC, Schmal H, Uhl M, Ghanem N, Sudkamp NP, Salzmann G (2014) Long-term outcomes after first-generation autologous chondrocyte implantation for cartilage defects of the knee. *Am J Sports Med* 42:150–157. <https://doi.org/10.1177/0363546513506593>
- Pelttari K, Winter A, Steck E, Goetzke K, Hennig T, Ochs BG, Aigner T, Richter W (2006) Premature induction of hypertrophy during in vitro chondrogenesis of human mesenchymal stem cells correlates with calcification and vascular invasion after ectopic transplantation in SCID mice. *Arthritis Rheum* 54:3254–3266. <https://doi.org/10.1002/art.22136>
- Fischer J, Dickhut A, Rickert M, Richter W (2010) Human articular chondrocytes secrete parathyroid hormone-related protein and inhibit hypertrophy of mesenchymal stem cells in coculture during chondrogenesis. *Arthritis Rheum* 62:2696–2706. <https://doi.org/10.1002/art.27565>
- Amizuka N, Warshawsky H, Henderson JE, Goltzman D, Karaplis AC (1994) Parathyroid hormone-related peptide-depleted mice show abnormal epiphyseal cartilage development altered endochondral bone-formation. *J Cell Biol* 126:1611–1623. <https://doi.org/10.1083/jcb.126.6.1611>
- Vortkamp A, Lee K, Lanske B, Segre GV, Kronenberg HM, Tabin CJ (1996) Regulation of rate of cartilage differentiation by Indian hedgehog and PTH-related protein. *Science* 273:613–622

10. Mueller MB, Tuan RS (2008) Functional characterization of hypertrophy in chondrogenesis of human mesenchymal stem cells. *Arthritis Rheum* 58:1377–1388
11. Narcisi R, Cleary MA, Brama PA, Hoogduijn MJ, Tuysuz N, Ten Berge D, van Osch GJ (2015) Long-term expansion, enhanced chondrogenic potential, and suppression of endochondral ossification of adult human MSCs via WNT signaling modulation. *Stem Cell Rep* 4:459–472. <https://doi.org/10.1016/j.stemcr.2015.01.017>
12. Yang Z, Zou Y, Guo XM, Tan HS, Denslin V, Yeow CH, Ren XF, Liu TM, Hui JH, Lee EH (2012) Temporal activation of beta-catenin signaling in the chondrogenic process of mesenchymal stem cells affects the phenotype of the cartilage generated. *Stem Cells Dev* 21:1966–1976. <https://doi.org/10.1089/scd.2011.0376>
13. Lolli A, Narcisi R, Lambertini E, Penolazzi L, Angelozzi M, Kops N, Gasparini S, van Osch GJ, Piva R (2016) Silencing of anti-chondrogenic MicroRNA-221 in human mesenchymal stem cells promotes cartilage repair in vivo. *Stem Cells* 34:1801–1811. <https://doi.org/10.1002/stem.2350>
14. Ng JJ, Wei Y, Zhou B, Bernhard J, Robinson S, Burapachaisri A, Guo XE, Vunjak-Novakovic G (2017) Recapitulation of physiological spatiotemporal signals promotes in vitro formation of phenotypically stable human articular cartilage. *Proc Natl Acad Sci USA* 114:2556–2561. <https://doi.org/10.1073/pnas.1611771114>
15. Occhetta P, Pigeot S, Rasponi M, Dasen B, Mehrkens A, Ullrich T, Kramer I, Guth-Gundel S, Barbero A, Martin I (2018) Developmentally inspired programming of adult human mesenchymal stromal cells toward stable chondrogenesis. *Proc Natl Acad Sci USA* 115:4625–4630. <https://doi.org/10.1073/pnas.1720658115>
16. Goldring MB, Tsuchimochi K, Ijiri K (2006) The control of chondrogenesis. *J Cell Biochem* 97:33–44. <https://doi.org/10.1002/jcb.20652>
17. Fischer J, Ortel M, Hagmann S, Hoefflich A, Richter W (2016) Role of PTHrP(1-34) pulse frequency versus pulse duration to enhance mesenchymal stromal cell chondrogenesis. *J Cell Physiol* 231:2673–2681. <https://doi.org/10.1002/jcp.25369>
18. Leijten JC, Emons J, Sticht C, van Gool S, Decker E, Uitterlinden A, Rappold G, Hofman A, Rivadeneira F, Scherjon S, Wit JM, van Meurs J, van Blitterswijk CA, Karperien M (2012) Gremlin 1, frizzled-related protein, and Dkk-1 are key regulators of human articular cartilage homeostasis. *Arthritis Rheum* 64:3302–3312. <https://doi.org/10.1002/art.34535>
19. Kronenberg HM (2003) Developmental regulation of the growth plate. *Nature* 423:332–336. <https://doi.org/10.1038/nature01657>
20. Pogue R, Lyons K (2006) BMP signaling in the cartilage growth plate. *Curr Top Dev Biol* 76:1–48. [https://doi.org/10.1016/S0070-2153\(06\)76001-X](https://doi.org/10.1016/S0070-2153(06)76001-X)
21. Dexheimer V, Gabler J, Bomans K, Sims T, Omlor G, Richter W (2016) Differential expression of TGF-beta superfamily members and role of Smad1/5/9-signalling in chondral versus endochondral chondrocyte differentiation. *Sci Rep* 6:36655. <https://doi.org/10.1038/srep36655>
22. Takegami Y, Ohkawara B, Ito M, Masuda A, Nakashima H, Ishiguro N, Ohno K (2016) R-spondin 2 facilitates differentiation of proliferating chondrocytes into hypertrophic chondrocytes by enhancing Wnt/beta-catenin signaling in endochondral ossification. *Biochem Biophys Res Commun* 473:255–264. <https://doi.org/10.1016/j.bbrc.2016.03.089>
23. Lu C, Wan Y, Cao J, Zhu X, Yu J, Zhou R, Yao Y, Zhang L, Zhao H, Li H, Zhao J, He L, Ma G, Yang X, Yao Z, Guo X (2013) Wnt-mediated reciprocal regulation between cartilage and bone development during endochondral ossification. *Bone* 53:566–574. <https://doi.org/10.1016/j.bone.2012.12.016>
24. Day TF, Guo X, Garrett-Beal L, Yang Y (2005) Wnt/beta-catenin signaling in mesenchymal progenitors controls osteoblast and chondrocyte differentiation during vertebrate skeletogenesis. *Dev Cell* 8:739–750. <https://doi.org/10.1016/j.devcel.2005.03.016>
25. Dao DY, Jonason JH, Zhang Y, Hsu W, Chen D, Hilton MJ, O'Keefe RJ (2012) Cartilage-specific beta-catenin signaling regulates chondrocyte maturation, generation of ossification centers, and perichondrial bone formation during skeletal development. *J Bone Miner Res* 27:1680–1694. <https://doi.org/10.1002/jbmr.1639>
26. Tamamura Y, Otani T, Kanatani N, Koyama E, Kitagaki J, Komori T, Yamada Y, Costantini F, Wakisaka S, Pacifici M, Iwamoto M, Enomoto-Iwamoto M (2005) Developmental regulation of Wnt/beta-catenin signals is required for growth plate assembly, cartilage integrity, and endochondral ossification. *J Biol Chem* 280:19185–19195. <https://doi.org/10.1074/jbc.M414275200>
27. Enomoto-Iwamoto M, Kitagaki J, Koyama E, Tamamura Y, Wu C, Kanatani N, Koike T, Okada H, Komori T, Yoneda T, Church V, Francis-West PH, Kurisu K, Nohno T, Pacifici M, Iwamoto M (2002) The Wnt antagonist Frzb-1 regulates chondrocyte maturation and long bone development during limb skeletogenesis. *Dev Biol* 251:142–156
28. Itasaki N, Hoppler S (2010) Crosstalk between Wnt and bone morphogenetic protein signaling: a turbulent relationship. *Dev Dyn* 239:16–33. <https://doi.org/10.1002/dvdy.22009>
29. Rawadi G, Vayssiere B, Dunn F, Baron R, Roman-Roman S (2003) BMP-2 controls alkaline phosphatase expression and osteoblast mineralization by a Wnt autocrine loop. *J Bone Miner Res* 18:1842–1853. <https://doi.org/10.1359/jbmr.2003.18.10.1842>
30. Zhang R, Oyajobi BO, Harris SE, Chen D, Tsao C, Deng HW, Zhao M (2013) Wnt/beta-catenin signaling activates bone morphogenetic protein 2 expression in osteoblasts. *Bone* 52:145–156. <https://doi.org/10.1016/j.bone.2012.09.029>
31. Intini G, Nyman JS (2015) Dkk1 haploinsufficiency requires expression of Bmp2 for bone anabolic activity. *Bone* 75:151–160. <https://doi.org/10.1016/j.bone.2015.01.008>
32. Baron R, Kneissel M (2013) WNT signaling in bone homeostasis and disease: from human mutations to treatments. *Nat Med* 19:179–192. <https://doi.org/10.1038/nm.3074>
33. Mak KK, Chen MH, Day TF, Chuang PT, Yang Y (2006) Wnt/beta-catenin signaling interacts differentially with Ihh signaling in controlling endochondral bone and synovial joint formation. *Development* 133:3695–3707. <https://doi.org/10.1242/dev.02546>
34. Spater D, Hill TP, O'Sullivan RJ, Gruber M, Conner DA, Hartmann C (2006) Wnt9a signaling is required for joint integrity and regulation of Ihh during chondrogenesis. *Development* 133:3039–3049. <https://doi.org/10.1242/dev.02471>
35. Najdi R, Proffitt K, Sprowl S, Kaur S, Yu J, Covey TM, Virshup DM, Waterman ML (2012) A uniform human Wnt expression library reveals a shared secretory pathway and unique signaling activities. *Differentiation* 84:203–213. <https://doi.org/10.1016/j.diff.2012.06.004>
36. Farndale RW, Buttle DJ, Barrett AJ (1986) Improved quantitation and discrimination of sulphated glycosaminoglycans by use of dimethylmethylene blue. *Biochim Biophys Acta* 883:173–177
37. Witte F, Dokas J, Neuendorf F, Mundlos S, Stricker S (2009) Comprehensive expression analysis of all Wnt genes and their major secreted antagonists during mouse limb development and cartilage differentiation. *Gene Expr Patterns* 9:215–223. <https://doi.org/10.1016/j.gep.2008.12.009>
38. Dy P, Wang W, Bhattaram P, Wang Q, Wang L, Ballock RT, Lefebvre V (2012) Sox9 directs hypertrophic maturation and blocks osteoblast differentiation of growth plate chondrocytes. *Dev Cell* 22:597–609. <https://doi.org/10.1016/j.devcel.2011.12.024>
39. Arnold MA, Kim Y, Czubyrt MP, Phan D, McAnally J, Qi X, Shelton JM, Richardson JA, Bassel-Duby R, Olson EN (2007) MEF2C transcription factor controls chondrocyte hypertrophy and bone development. *Dev Cell* 12:377–389. <https://doi.org/10.1016/j.devcel.2007.02.004>

40. Stephens AS, Stephens SR, Hobbs C, Hutmacher DW, Bacic-Welsh D, Woodruff MA, Morrison NA (2011) Myocyte enhancer factor 2c, an osteoblast transcription factor identified by dimethyl sulfoxide (DMSO)-enhanced mineralization. *J Biol Chem* 286:30071–30086. <https://doi.org/10.1074/jbc.M111.253518>
41. Miyazono K, Miyazawa K (2002) Id: a target of BMP signaling. *Sci STKE* 2002:pe40. <https://doi.org/10.1126/stke.2002.151.pe40>
42. Hollnagel A, Oehlmann V, Heymer J, Ruther U, Nordheim A (1999) Id genes are direct targets of bone morphogenetic protein induction in embryonic stem cells. *J Biol Chem* 274:19838–19845
43. Fischer J, Aulmann A, Dexheimer V, Grossner T, Richter W (2014) Intermittent PTHrP(1–34) exposure augments chondrogenesis and reduces hypertrophy of mesenchymal stromal cells. *Stem Cells Dev* 23:2513–2523. <https://doi.org/10.1089/scd.2014.0101>
44. Andrade AC, Nilsson O, Barnes KM, Baron J (2007) Wnt gene expression in the post-natal growth plate: regulation with chondrocyte differentiation. *Bone* 40:1361–1369. <https://doi.org/10.1016/j.bone.2007.01.005>
45. Church V, Nohno T, Linker C, Marcelle C, Francis-West P (2002) Wnt regulation of chondrocyte differentiation. *J Cell Sci* 115:4809–4818
46. Lee HH, Behringer RR (2007) Conditional expression of Wnt4 during chondrogenesis leads to dwarfism in mice. *PLoS One* 2:e450. <https://doi.org/10.1371/journal.pone.0000450>
47. Dexheimer V, Frank S, Richter W (2012) Proliferation as a requirement for in vitro chondrogenesis of human mesenchymal stem cells. *Stem Cells Dev* 21:2160–2169. <https://doi.org/10.1089/scd.2011.0670>
48. Huang X, Zhong L, Hendriks J, Post JN, Karperien M (2018) The effects of the WNT-signaling modulators BIO and PKF118-310 on the chondrogenic differentiation of human mesenchymal stem cells. *Int J Mol Sci*. <https://doi.org/10.3390/ijms19020561>
49. Im GI, Lee JM, Kim HJ (2011) Wnt inhibitors enhance chondrogenesis of human mesenchymal stem cells in a long-term pellet culture. *Biotechnol Lett* 33:1061–1068. <https://doi.org/10.1007/s10529-010-0514-3>
50. Zhu X, Zhu H, Zhang L, Huang S, Cao J, Ma G, Feng G, He L, Yang Y, Guo X (2012) Wls-mediated Wnts differentially regulate distal limb patterning and tissue morphogenesis. *Dev Biol* 365:328–338. <https://doi.org/10.1016/j.ydbio.2012.02.019>
51. Hartmann C, Tabin CJ (2000) Dual roles of Wnt signaling during chondrogenesis in the chicken limb. *Development* 127:3141–3159
52. Yang Y, Topol L, Lee H, Wu J (2003) Wnt5a and Wnt5b exhibit distinct activities in coordinating chondrocyte proliferation and differentiation. *Development* 130:1003–1015
53. Yamaguchi TP, Bradley A, McMahon AP, Jones S (1999) A Wnt5a pathway underlies outgrowth of multiple structures in the vertebrate embryo. *Development* 126:1211–1223
54. Albanese I, Yu B, Al-Kindi H, Barratt B, Ott L, Al-Refai M, de Varennes B, Shum-Tim D, Cerruti M, Gourgas O, Rheaume E, Tardif JC, Schwertani A (2017) Role of noncanonical Wnt signaling pathway in human aortic valve calcification. *Arterioscler Thromb Vasc Biol* 37:543–552. <https://doi.org/10.1161/ATVBAHA.116.308394>
55. Friedman MS, Oyserman SM, Hankenson KD (2009) Wnt11 promotes osteoblast maturation and mineralization through R-spondin 2. *J Biol Chem* 284:14117–14125. <https://doi.org/10.1074/jbc.M808337200>
56. Liu S, Zhang E, Yang M, Lu L (2014) Overexpression of Wnt11 promotes chondrogenic differentiation of bone marrow-derived mesenchymal stem cells in synergism with TGF-beta. *Mol Cell Biochem* 390:123–131. <https://doi.org/10.1007/s11010-014-1963-0>
57. Fukuda T, Kokabu S, Ohte S, Sasanuma H, Kanomata K, Yoneyama K, Kato H, Akita M, Oda H, Katagiri T (2010) Canonical Wnts and BMPs cooperatively induce osteoblastic differentiation through a GSK3beta-dependent and beta-catenin-independent mechanism. *Differentiation* 80:46–52. <https://doi.org/10.1016/j.diff.2010.05.002>
58. Glinka A, Delius H, Blumenstock C, Niehrs C (1996) Combinatorial signalling by Xwnt-11 and Xnr3 in the organizer epithelium. *Mech Dev* 60:221–231. [https://doi.org/10.1016/S0925-4773\(96\)00624-7](https://doi.org/10.1016/S0925-4773(96)00624-7)
59. Zhang P, Cai Y, Soofi A, Dressler GR (2012) Activation of Wnt11 by transforming growth factor-beta drives mesenchymal gene expression through non-canonical Wnt protein signaling in renal epithelial cells. *J Biol Chem* 287:21290–21302. <https://doi.org/10.1074/jbc.M112.357202>
60. Liu J, Johnson K, Li J, Piamonte V, Steffy BM, Hsieh MH, Ng N, Zhang J, Walker JR, Ding S, Muneoka K, Wu X, Glynne R, Schultz PG (2011) Regenerative phenotype in mice with a point mutation in transforming growth factor beta type I receptor (TGFBRI). *Proc Natl Acad Sci USA* 108:14560–14565. <https://doi.org/10.1073/pnas.1111056108>
61. Chen B, Dodge ME, Tang W, Lu J, Ma Z, Fan CW, Wei S, Hao W, Kilgore J, Williams NS, Roth MG, Amatruda JF, Chen C, Lum L (2009) Small molecule-mediated disruption of Wnt-dependent signaling in tissue regeneration and cancer. *Nat Chem Biol* 5:100–107. <https://doi.org/10.1038/nchembio.137>
62. Weiss S, Hennig T, Bock R, Steck E, Richter W (2010) Impact of growth factors and PTHrP on early and late chondrogenic differentiation of human mesenchymal stem cells. *J Cell Physiol* 223:84–93. <https://doi.org/10.1002/jcp.22013>
63. Gabler J, Ruetze M, Kynast KL, Grossner T, Diederichs S, Richter W (2015) Stage-specific miRs in chondrocyte maturation: differentiation-dependent and hypertrophy-related miR clusters and the miR-181 family. *Tissue Eng Part A* 21:2840–2851. <https://doi.org/10.1089/ten.TEA.2015.0352>
64. Rasini V, Dominici M, Kluba T, Siegel G, Lusenti G, Northoff H, Horwitz EM, Schafer R (2013) Mesenchymal stromal/stem cells markers in the human bone marrow. *Cytherapy*. <https://doi.org/10.1016/j.jcyt.2012.11.009>
65. Sacchetti B, Funari A, Michienzi S, Di Cesare S, Piersanti S, Saggio I, Tagliafico E, Ferrari S, Robey PG, Riminucci M, Bianco P (2007) Self-renewing osteoprogenitors in bone marrow sinusoids can organize a hematopoietic microenvironment. *Cell* 131:324–336. <https://doi.org/10.1016/j.cell.2007.08.025>
66. Brocher J, Janicki P, Voltz P, Seebach E, Neumann E, Mueller-Ladner U, Richter W (2013) Inferior ectopic bone formation of mesenchymal stromal cells from adipose tissue compared to bone marrow: rescue by chondrogenic pre-induction. *Stem Cell Res* 11:1393–1406. <https://doi.org/10.1016/j.scr.2013.07.008>

Publisher's Note Springer Nature remains neutral with regard to jurisdictional claims in published maps and institutional affiliations.